

1 **1 Aminated Poly(Ethylene Glycol) Methacrylate Resins as**
2 **Stable Heterogeneous Catalysts for the Aldol Reaction in**
3 **Water**

4 *Anton De Vyllder^a, Jeroen Lauwaert^b, Jeriffa De Clercq^b, Pascal Van Der Voort^c,*

5 *Christopher W. Jones^d, Joris W. Thybaut^{a,*}*

6 ^aLaboratory for Chemical Technology (LCT), Department of Materials, Textiles, and Chemical
7 Engineering, Ghent University, Technologiepark 125, 9052 Ghent, Belgium

8 ^bIndustrial Catalysis and Adsorption Technology (INCAT), Department of Materials, Textiles,
9 and Chemical Engineering, Ghent University, Valentin Vaerwyckweg 1, 9000 Ghent, Belgium

10 ^cCenter for Ordered Materials, Organometallics and Catalysis (COMOC), Department of
11 Chemistry, Ghent University, Krijgslaan 281-S3, 9000 Ghent, Belgium

12 ^dGeorgia Institute of Technology, School of Chemical & Biomolecular Engineering, 311 Ferst
13 Drive, Atlanta, GA 30332-0100, USA

14

15 **Abstract**

16 Amine functionalized silicas have frequently been investigated as potential aldol reaction
17 catalysts. However, active site leaching due to hydrolysis cannot be avoided as a limiting factor
18 for the long-term stability of these catalysts in aqueous aldol reactions. Therefore, novel catalysts
19 based on an organic resin have been developed starting from a suspension polymerized
20 poly(ethylene glycol) methacrylate (PEGMA) hydrogel with poly(ethylene glycol)
21 dimethacrylate (PEGDMA) as cross-linker. Amine functionalization was performed by
22 chlorination of the terminal hydroxyl groups in the resulting PEGMA resin and subsequent
23 nucleophilic substitution with an amine precursor, *i.e.*, ethylenediamine (EDA),
24 N,N'-dimethylethylenediamine (DED), or methylamine (MA). The successful synthesis of the
25 catalysts was confirmed by ¹³C-NMR, FT-IR, and elemental CHN analysis. Performance
26 evaluation in a batch reactor for the aqueous aldol reaction of acetone with 4-nitrobenzaldehyde
27 resulted in a turnover frequency (TOF) of the PEGMA-EDA catalyst amounting to
28 $6.3 \pm 0.4 \cdot 10^{-4} \text{ s}^{-1}$, which is of the same order of magnitude as that of the corresponding state-of-
29 the-art amine functionalized silica evaluated using hexane as solvent. The PEGMA-DED catalyst
30 exhibited a somewhat lower TOF of $3.1 \pm 0.2 \cdot 10^{-4} \text{ s}^{-1}$, while the PEGMA-MA catalyst did not
31 exhibit any turnover, indicating that the secondary amine in the backbone of the active site in the
32 PEGMA-EDA catalyst is inactive. Continuous-flow evaluation of the PEGMA-EDA catalyst in a
33 packed-bed reactor indicated that, as opposed to a primary amine functionalized silica catalyst, a
34 stable catalytic activity as a function of time on stream could be achieved for at least 8 hours and,
35 hence, that no deactivation has occurred in this timeframe.

36

37 **Keywords:** Aminated PEGMA, Aldol Reaction, Heterogeneous Catalysis, Water,
38 Continuous-Flow

39 **2 Introduction**

40 Aldol reactions establish carbon-carbon bonds between two carbonyl-containing species and are
41 widely used to synthesize more complex organic molecules from simpler ones. They are
42 typically used in the synthesis of fine chemical [1] and pharmaceutical [2] components. A
43 potential new application is situated in the bio-based industry for the production of liquid fuels
44 from lignocellulosic biomass resources [3]. At present, commercially implemented aldol
45 reactions are typically catalyzed by homogeneous strong bases. Despite their adequate activity,
46 these catalysts are dangerous to handle, pose an environmental risk, and are deactivated upon
47 separation from the product stream [1]. Heterogeneous alternative catalysts with primary or
48 secondary amine sites, particularly those grafted on a mesoporous silica surface, have often been
49 investigated for the model aldol reaction of acetone with 4-nitrobenzaldehyde [4-9]. Secondary
50 amines are generally preferred as active sites when the reaction is performed in an organic
51 solvent, because on primary amines, stable imines of both 4-nitrobenzaldehyde and acetone can
52 form in substantial amounts, leading to active site inhibition, and tertiary amines cannot form the
53 crucial enamine intermediate [4, 7]. With secondary amines, care should also be taken that the
54 substituent does not cause a too large steric hindrance [4, 10]. Hence, the methylaminopropyl
55 functional group is currently reported as resulting in the highest activity [4]. With water as
56 solvent, imine formation on primary amines was found to be less of an issue [11, 12]. In turn, the
57 formation of an inhibiting stable iminium ion on secondary amines has been hypothesized to
58 occur to a significant extent in an aqueous environment, resulting in primary amines actually
59 outperforming secondary amines [11]. Water is also attractive as solvent, because it is cheap,
60 readily available and not toxic [13]. However, the current state-of-the-art amine functionalized
61 silica catalysts are not stable in water, due to the hydrolysis of Si-O-Si bonds [14, 15], which
62 results in structural degradation of the mesoporous silica material and active site leaching [16].

63 There is, hence, a need for more hydrothermally stable heterogeneous amine catalysts for
64 application in aqueous aldol reactions.

65 Organic support materials do not contain any Si-O-Si bonds and will thus not be subjected to the
66 same hydrolysis reactions as silica-based materials. Polystyrene is an example of a polymer for
67 which a plethora of different supported L-proline catalysts have already been developed and
68 evaluated in the aqueous aldol reaction [17-24]. Polystyrene is chosen as polymer support for
69 these catalysts, because a hydrophobic environment could be created around L-proline, which is
70 otherwise inactive in water [19, 25]. However, no clear information has been reported about the
71 stability of these catalysts, as it is often not reported at all or only reported at complete reagent
72 conversion in repeat batch experiments, which does not provide information about the kinetics of
73 deactivation [26-28]. Other types of amine functionalized organic catalysts, e.g., with
74 intermolecular promoting groups, have also been developed. Hoyt et al. [29] synthesized
75 cooperative acid-base polystyrene polymers with primary amines that were promoted by
76 neighboring hydroxyl or carboxylic acid groups. However, the hydrophobic polymer material
77 could not sufficiently swell in the reaction environment, which resulted in a poor accessibility of
78 the catalytic sites. More recently, Ellebracht et al. [30, 31] used cellulose nanocrystals as organic
79 support to create either monofunctional primary amine catalysts, or amine catalysts that are
80 intermolecularly promoted by cooperative acid groups. However, relatively slow aldol reactions
81 were achieved in water/acetone reaction mixtures for the unpromoted catalyst [30]. The
82 promoted catalysts, which were evaluated in an acetonitrile/acetone solvent mixture, exhibited a
83 much higher activity but a poor recyclability [31], likely due to a strong binding of 4-
84 nitrobenzaldehyde in the form of imines on the active site. Recent work has also shown that the
85 primary amines, present in the biopolymer chitosan, are stable in the aqueous aldol reaction but

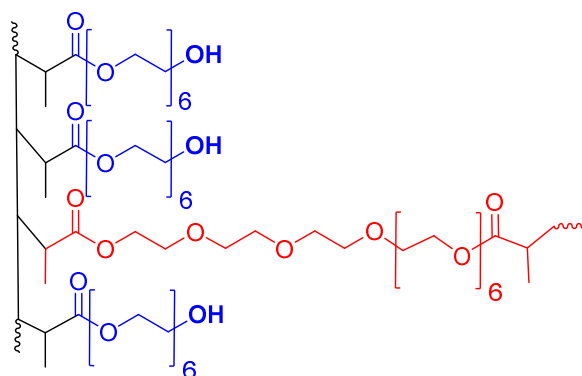
86 lack an adequate activity [32]. The currently available heterogeneous aminated polymer based
87 catalysts are, hence, either unstable or exhibit a poor activity as compared to the silica-based
88 materials.

89 In this work, a stable heterogeneous amine functionalized hydrophilic organic resin is developed.

90 A tailored extent of cross-linking ensures that the polymer does not dissolve in the reaction
91 mixture, while preserving the possibility to swell and as such guarantee the active sites
92 accessibility [33]. However, to adequately swell in the reaction mixture, which is in this case a
93 mixture of water as solvent and acetone as excess reagent, it is vital that the polymer is
94 hydrophilic. Hence, the catalysts are based on polyethylene glycol (PEG), which is described as
95 a “chameleon type” polymer, because it has both hydrophobic and hydrophilic properties [34].

96 As a crosslinked resin, it will swell in water, acetone, ethanol as well as toluene, methylene
97 chloride, and many organic solvents [34]. This versatile swelling behavior allows to efficiently
98 synthesize the catalyst in a dry organic solvent, while allowing the use of its catalytic properties
99 in the aqueous aldol reaction. Combined with its stability under the typical reaction conditions
100 used in the aldol reaction [35], and easy functionalization [36], PEG derived catalysts appear
101 very attractive.

102 PEG polymers with an average Mn between 360 and 520 and one or two methacrylate endgroups
103 are commercially available, and are respectively denoted as poly(ethylene glycol) methacrylate
104 (PEGMA) or poly(ethylene glycol) dimethacrylate (PEGDMA). A combination of these
105 monomers will then be polymerized via the methacrylate functions into resins via a free-radical
106 suspension polymerization [37]. The endgroups of these polymers are hydroxyl groups, as
107 displayed in Figure 1.



108

109 **Figure 1:** Resins based on a poly(ethylene glycol) methacrylate (average $M_n = 360$, 6 PEG units) and
 110 cross-linked with a poly(ethylene glycol) dimethacrylate (average $M_n = 750$, 9 PEG units)

111

112 3 Procedures

113

114 3.1 Synthesis and characterization of PEGMA catalysts

115

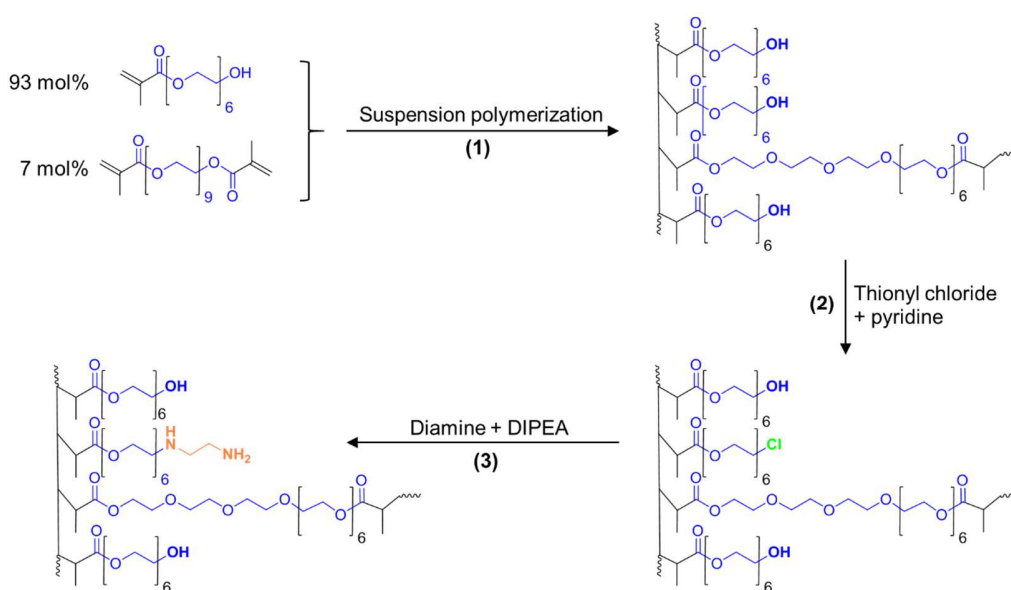
116 The first step in the catalyst preparation is the synthesis of a cross-linked poly(ethylene glycol)
 117 methacrylate resin as displayed in Figure 1. This synthesis occurs via a suspension
 118 polymerization, displayed in Scheme 1, step 1, as described by Tuncel et al. [37] A stabilizer,
 119 PVP (Sigma-Aldrich, K30, MW 40000) is dissolved in 40 mL deionized water for the
 120 preparation of the continuous phase. The disperse phase was prepared by mixing 5.5 mL
 121 cyclohexanol (Sigma-Aldrich, ReagentPlus, 99%) with 2.0 mL octanol (Acros, 99%), 4.0 mL
 122 poly(ethylene glycol) methacrylate (Sigma-Aldrich, average M_n 360) and 0.6 mL poly(ethylene
 123 glycol) dimethacrylate (Sigma-Aldrich, average M_n 750). The initiator BPO (0.12 g, Luperox®
 124 A98, reagent grade, $\geq 98\%$) was then dissolved in this homogeneous solution. The disperse phase
 125 was added to the continuous phase in a 50 mL glass flask and stirred at 450 rpm for 4 hours at 85
 126 °C and for 1 hour at 90 °C. After completion, swellable resin beads were obtained which were
 127 washed twice with acetone (VWR, 99.5%) and dried overnight on a high vacuum line at 50 °C.

128 In the next step, the dried hydrogel beads were covered completely with 40 mL dry toluene
129 (Sigma-Aldrich, anhydrous, 99,8%), 0.3 mL of thionyl chloride (Sigma-Aldrich, >99%,
130 ReagentPlus) was added and 0.33 mL pyridine (JT Baker, ACS Reagent, 100%). The targeted
131 chlorine loading was 0.81 mmol g⁻¹, corresponding to a 30% replacement of the hydroxyl
132 groups. This mixture was stirred for 4 hours at 75 °C before being filtered off, washed twice in
133 ethanol (Koptec, 200 proof), and dried overnight on a high vacuum line at 50 °C. To produce a
134 100% chlorine substituted material (100-PEGMA-Cl), which, in section 3.1 is used to ensure a
135 higher resolution in the characterization steps, 1.0 mL of thionyl chloride and 1.1 mL of pyridine
136 was used.

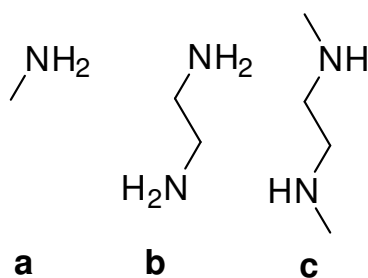
137 Finally, in the last step in Scheme 1, amine and diamines as displayed in Figure 2 are introduced
138 on the material by S_N2 nucleophilic substitution of the chlorine group. For this, either 5 mL
139 ethylenediamine (Sigma-Aldrich, 99%, ReagentPlus) or 3 mL N,N'-dimethylethylenediamine
140 (Alfa Aesar, 95%) or 15 mL methylamine (2.0 M in THF, Sigma Aldrich) is added to the resin
141 beads dissolved in dry toluene. An equivalent molar amount of di-isopropylethylamine (DIPEA,
142 Sigma-Aldrich, >99%, ReagentPlus) is added as HCl scavenger. Grafting of the diamines is
143 performed at reflux temperature (110 °C) for 24 hours, grafting of methylamine is performed at
144 40 °C for 48 hours. Afterwards, the obtained catalysts are washed twice in 200 mL ethanol and
145 dried at 50 °C on a high vacuum. To obtain a highly functionalized PEGMA-EDA material,
146 which will not be catalytically evaluated but is used in section 3.1 to obtain a material with a
147 high resolution for characterization, 25 mL of ethylenediamine (Sigma-Aldrich, 99%,
148 ReagentPlus) was used.

149 CHN analysis of PEGMA catalysts was performed by Atlantic MicroLabs. The active site
150 loading is determined as the concentration of amine groups for the methylamine functionalized

151 catalyst (PEGMA-MA), and half of the concentration of amine groups for the diamines
 152 (PEGMA-EDA and PEGMA-DED). Non-spinning Direct Polarization (DP) ^{13}C Nuclear
 153 Magnetic Resonance (NMR) spectra were recorded at 60 °C with a Bruker AVIII-300. Fourier
 154 Transform-Infrared (FT-IR) transmission spectroscopy was performed with a Nicolet iS10
 155 Spectrometer. SEM images of the resin beads were collected with a Hitachi SU 8010 scanning
 156 electron microscope.



157
 158 **Scheme 1:** Synthesis procedure of PEGMA catalysts, in this example functionalized with a primary
 159 ethylenediamine (PEGMA-EDA). Other amines or diamines can also be used in the same procedure.



160
 161 **Figure 2:** Amines used for functionalization of 30-PEGMA-Cl, a) methylamine (MA), b)
 162 ethylenediamine (EDA), c) N,N'-dimethylethylenediamine (DED)

163

164 2.2 Synthesis and characterization of the aminated mesoporous silica catalyst

165

166 To compare the stability of the developed PEGMA resin catalyst to the state-of-the-art
167 aminated mesoporous silica, a primary amine functionalized mesoporous silica catalyst (Silica-
168 APS) was synthesized according to the well-known literature procedures [4, 7, 16, 38]. Silicagel
169 60 (grade 7734, Sigma-Aldrich, pellet diameter between 250 μm and 500 μm) was first heated to
170 700 $^{\circ}\text{C}$ (heating rate of 2 $^{\circ}\text{C min}^{-1}$) and kept at this temperature for 6 hours. Afterwards, the
171 silica support is cooled to 120 $^{\circ}\text{C}$ and 5g is diluted in 30 mL toluene (extra dry, Acros). Next, the
172 silane (3-aminopropyl)triethoxysilane (98%, APTES, ABCR) is added with a targeted amine
173 loading of 0.3 mmol g^{-1} . The volume of silane required is calculated by assuming the number of
174 free silanols equals 1.1 OH nm^{-2} after calcination at 700 $^{\circ}\text{C}$ [39]. Subsequently, the mixture is
175 refluxed at 110 $^{\circ}\text{C}$ for 24 hours under an argon atmosphere. Filtration is then performed to
176 recover the solid sample, followed by washing with chloroform (>99.8%, Roth, <50 ppm H_2O)
177 and drying in vacuum for 24 hours at room temperature.

178 The concentration of amine groups, corresponding to the concentration of active sites, was
179 determined via elemental (CHN) analysis. These measurements were performed on a Thermo
180 Flash 2000 elemental analyzer using V_2O_5 as catalyst, in order to ensure the total oxidation of the
181 sample. The mass percentage of nitrogen in the sample is obtained by referring the obtained peak
182 area to a calibration curve of methionine (USP, 99%) that was obtained prior to the
183 measurements.

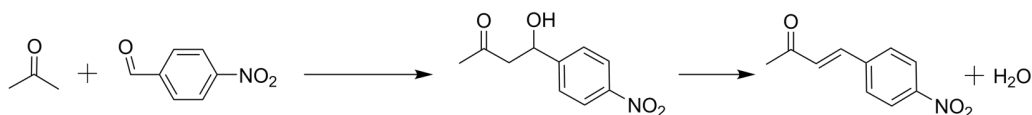
184

185 2.3 Performance Evaluation

186

187 The catalyst performance is evaluated for the aldol reaction of acetone (99.6%, Acros) with
188 4-nitrobenzaldehyde (99%, Acros), resulting in 4-hydroxy-4-(4-nitrophenyl)butan-2-one as aldol

189 product and 4-(4-nitrophenyl)-3-buten-2-one as enone product, see Scheme 2. This reaction was
190 selected because it is the typical benchmark aldol reaction [6, 38, 40] of which the effects of
191 solvent [11], water [16], type of active site [7] and cooperative effects [4] are well-known.



193 **Scheme 2:** Aldol reaction of acetone and 4-nitrobenzaldehyde towards the aldol product 4-hydroxy-4-(4-
194 nitrophenyl)butan-2-one, and dehydration to the enone product 4-(4-nitrophenyl)-3-buten-2-one.

195

196 2.3.1 Batch reactor

197

198 The catalyst performance was initially evaluated in a batch-type reactor (Parr 4560 mini, 300
199 mL), of which the procedure has been reported in previous work [4, 16]. The reactor was loaded
200 with an amount of catalyst equivalent with 0.06 mmol active amine sites, 55 g water as solvent
201 and 0.25 g methyl 4-nitrobenzoate (> 99%, Sigma-Aldrich) as internal standard. This mixture
202 was then heated to 55 °C, under constant stirring. Acetone (45 g) was separately heated to 55 °C
203 and was used to dissolve 0.45 g 4-nitrobenzaldehyde prior to injection in the reactor. The
204 reaction mixture was mechanically stirred at 400 rpm. The time of injection was taken as the
205 start of the reaction ($t = 0$). The reaction was monitored for 240 minutes by taking a sample (0.3
206 mL) of the reaction mixture every 15 minutes during the first hour and, subsequently, every 30
207 minutes for the remaining 3 hours. For each experiment, the total decrease of reaction volume
208 due to sampling was less than 5% whereby the effect of sampling on the kinetic data is
209 considered to be negligible. The turnover frequency (TOF) in the batch reactor was determined
210 from the slope of the initial linear part of the conversion of 4-nitrobenzaldehyde as a function of

211 reaction time, the concentration of active amine sites and the initial concentration of
212 4-nitrobenzaldehyde [28].

213

214 2.3.2 Continuous-flow reactor

215

216 The stability of the PEGMA-EDA and aminated mesoporous silica catalyst was evaluated in a
217 plug-flow reactor [28], of which the operating procedure has been reported in previous work
218 [16], with a site time of $544 \text{ mol}_{\text{site}} \text{ s mol}_{4\text{NB}}^{-1}$. Before loading into the reactor, the PEGMA resin
219 catalyst was swollen in deionized water for 30 minutes. The feed mixture was composed of 0.45
220 wt% 4-nitrobenzaldehyde, 44.6 wt% acetone, 54.5 wt% water and 0.25 wt% methyl-4-
221 nitrobenzoate as internal standard.

222

223 2.3.3 Sample analysis

224

225 The reaction samples were analyzed using a reversed-phase high-performance liquid
226 chromatograph (RP-HPLC), from Agilent (1100 series) on a XDB-C18 column [16]. The HPLC
227 was operated at 30 °C using a gradient method with water (0.1% trifluoroacetic acid, Acros) and
228 30 v% to 62 v% acetonitrile (HPLC grade, Acros) as solvents. This method separates all the
229 components in a period of 14 min. The components were identified using a UV-detector with a
230 variable wavelength that has been programmed for an optimal absorption for each component.
231 Quantification of the different components in the reaction mixture was performed by relating the
232 peak surface areas of the components to the amount and peak area of the internal standard added
233 to the reactor.

234 **4 Results and Discussion**

235

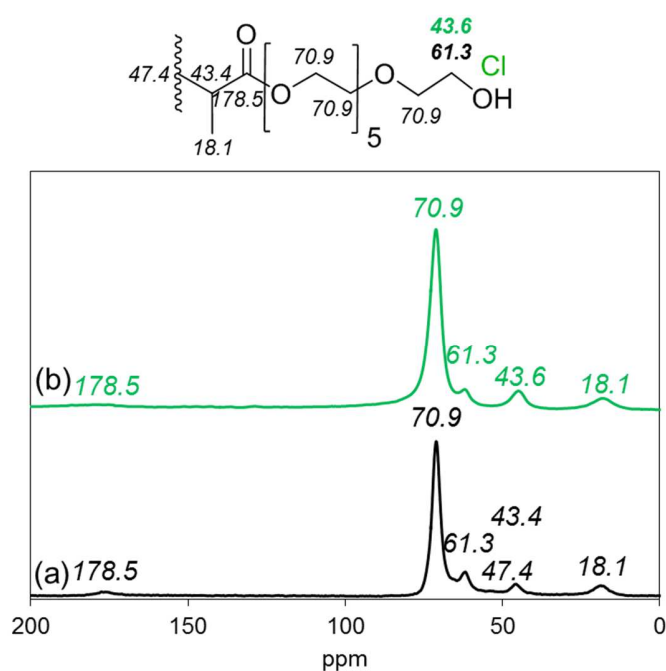
236 4.1 Catalyst characterization and validation of synthesis procedure

237

238 SEM images of the PEGMA resin beads are displayed in Figure 1S in the Supplementary
239 Information and indicate that spherical beads in the order of 100 μm are indeed formed in the
240 suspension polymerization. As indicated in Figure 3(a), the DP ^{13}C -NMR of the pristine resin
241 exhibits all the characteristic peaks of polymerized PEGMA, even though the peaks at 43.4 ppm
242 and 47.4 ppm appear to be overlapping and are not individually distinguishable. The first
243 functionalization step is the reaction with thionylchloride, which, as can be observed in Figure 3
244 (b), reduces the intensity of the peak at 61.3 ppm, corresponding to a carbon attached to a
245 hydroxyl group, and increases the peak around 43.6 ppm, corresponding to a carbon attached to
246 Cl. There is some overlap with the peak related to the polymerized methacrylate carbon atom at
247 47.4 ppm, but a clear shift in the maximum and intensity was found after chlorination. No other
248 peaks have shifted, or appeared. For comparative purposes, the ^{13}C -NMR spectrum of a 100%
249 chlorinated PEGMA material is given in the Supplementary Information Figure 2S. It is evident
250 from this figure that the peak of a carbon attached to a hydroxyl group, at 61.3 ppm, has entirely
251 disappeared in favor of a larger peak at 43.6 ppm corresponding to C-Cl. While such a highly
252 functionalized material is not used for catalytic purposes, it indicates that the resin can
253 sufficiently swell in dry toluene to allow access to all the hydroxyl sites.

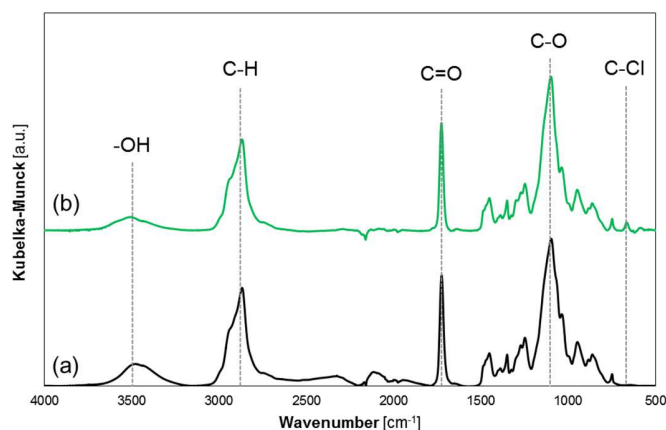
254 The FT-IR spectrum in Figure 4 supports the conclusions drawn above. The characteristic peaks
255 associated with the C-H, C=O and C-O vibrations in the polymerized PEGMA molecule are the
256 most intense and respectively appear at 2900 cm^{-1} , 1720 cm^{-1} and 1100 cm^{-1} in Figure 4(a). The
257 spectrum of the partially chlorinated 30-PEGMA-CL in Figure 4(b) shows that the peak

258 associated with hydroxyl groups in PEGMA, around 3500 cm^{-1} , reduces upon reaction with
259 thionyl chloride in favor of a C-Cl peak at 660 cm^{-1} . The spectrum of a 100% chlorinated
260 PEGMA material, as displayed in the Supplementary Information Figure 3S, indicates a
261 complete loss of the hydroxyl groups in PEGMA, around 3500 cm^{-1} and an increase in the C-Cl
262 peak at 660 cm^{-1} . No other peaks have appeared or changed shape. There is, hence, no obvious
263 indication that any other than the desired reaction occurred.



264
265
266

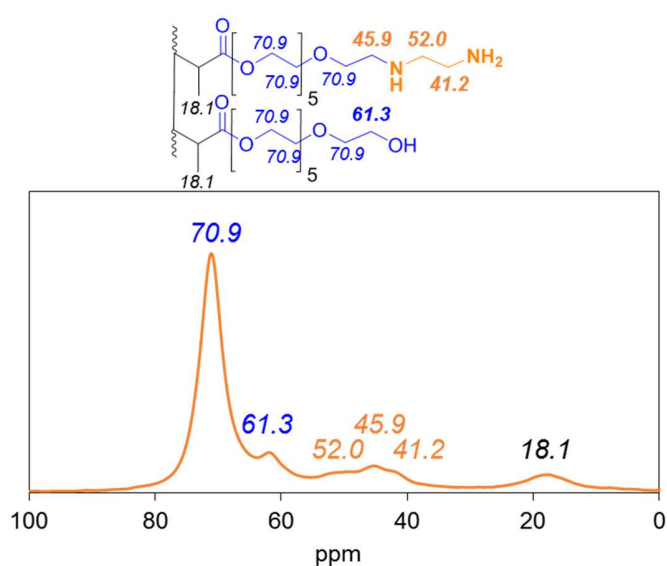
Figure 3: DP ^{13}C -NMR spectra at $60\text{ }^\circ\text{C}$ of PEGMA hydrogel (a) and the 30% chlorine functionalized hydrogel (30-PEGMA-Cl) (b)



267
 268 **Figure 4:** FT-IR spectra of the PEGMA resin (a) and the 30% chlorine functionalized 30-PEGMA-Cl (b)

269
 270 Next, the partially chlorine functionalized 30-PEGMA-Cl materials were subject to nucleophilic
 271 substitution with a symmetrical diamine to produce the desired catalysts. Reaction with
 272 ethylenediamine (EDA) resulted in the PEGMA-EDA catalyst, reaction with
 273 N,N'-dimethylethylenediamine (DED) resulted in the PEGMA-DED catalyst. The achieved
 274 loading is reported in Table 1. While the active site loadings are lower than the targeted loading,
 275 the obtained catalysts do allow to assess and compare the activity and stability of the amine sites
 276 in the aldol reaction. Figure 5 and Figure 6 respectively show the DP ^{13}C -NMR results of the
 277 PEGMA-EDA and PEGMA-DED catalysts including the peak assignment to the functionalized
 278 groups. While there appear peaks in the expected region in the ^{13}C -NMR profile, different
 279 individual assignment is difficult due to their low intensity. This is due to the relatively low
 280 diamine loading ($\sim 0.3 \text{ mmol g}^{-1}$) of the catalysts. The same issue causes the FT-IR spectra of the
 281 PEGMA-EDA and PEGMA-DED catalysts to be indistinguishable from the unfunctionalized
 282 PEGMA material, as displayed in the Supplementary Information Figure 4S. However, ^{13}C -
 283 NMR and FT-IR characterization results of a high-loaded PEGMA-EDA, with a 2.1 mmol g^{-1}
 284 diamine loading corresponding to 88% of the available hydroxyl groups being replaced with

285 EDA, are displayed in Figure 5S and Figure 6S. The peaks associated with the primary diamine
286 of this high-loaded material are clearly visible in the spectra. Even though this high-loaded
287 material is not evaluated for its catalytic activity because the amine groups would severely
288 sterically hinder each other, it indicates that the desired functionalization indeed occurs under the
289 employed experimental conditions and that there is no indication of undesired side-reactions
290 taking place.



291

292

Figure 5: DP ^{13}C -NMR spectra of the PEGMA-EDA catalyst at 60 °C

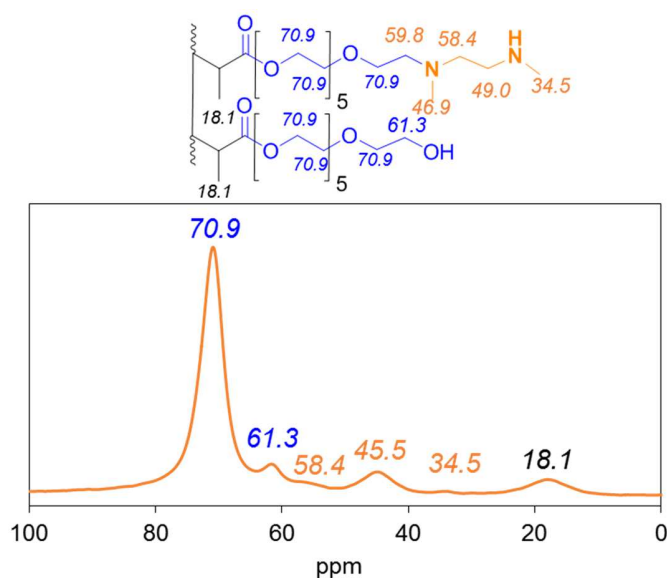


Figure 6: DP ^{13}C -NMR spectra of the PEGMA-DED catalyst at 60 °C

293

294

295

296 In order to investigate the possible catalytic activity of the secondary amine in the EDA chain of
 297 the PEGMA-EDA catalyst, functionalization with methylamine (MA) is also performed to
 298 produce PEGMA-MA. In the DP ^{13}C -NMR and FT-IR spectra corresponding to this material, no
 299 clear peaks relating to the methylamine group can be distinguished due to the low mass
 300 percentage of methylamine and the low intensity of secondary amine vibrations in FT-IR.
 301 However, its loading as determined from the nitrogen elemental analysis is reported in Table 1
 302 and proves that amine functionalization has occurred.

303 To compare the stability of the developed catalysts against the state-of-the-art amine
 304 functionalized silica catalysts, a primary amine functionalized silica catalyst (Silica-APS) is
 305 synthesized according to literature procedures [4] and its active site loading is also reported in
 306 Table 1.

307 **Table 1:** Active site loading for the PEGMA catalysts and the state-of-the-art aminated mesoporous silica
308 catalyst, determined with elemental CHN analysis. In case of diamines, the elemental nitrogen loading is
309 divided by two.

Catalyst	Active site loading $\pm 5\%$ (mmol g ⁻¹)
PEGMA-EDA	0.43
PEGMA-DED	0.28
PEGMA-MA	0.24
Silica-APS	0.26

310

311

312 4.2 Performance evaluation

313

314 Experiments with methylamine functionalized PEGMA-MA yielded no measurable
315 4-nitrobenzaldehyde conversion, as reported in Table 2. This indicates that the secondary amine,
316 which is formed at the anchoring point to the PEGMA backbone material in the PEGMA-EDA
317 catalyst, is not catalytically active. This is possibly related to the severe steric hindrance that is
318 encountered by the amine site from the neighboring PEG chains. Nucleophilic substitution with
319 N,N'-dimethylenediamine generated a tertiary amine which is known not to be active due to its
320 inability to form an enamine intermediate [4]. Hence, the only catalytically active sites on the
321 PEGMA-EDA and PEGMA-DED catalysts are, respectively, the terminal primary amine and the
322 terminal secondary amine.

323 Both the PEGMA-EDA and PEGMA-DED catalysts are evaluated for the aldol reaction in a
324 batch reactor and their activity curves are displayed in Figure 7S in the Supplementary
325 Information. The TOF exhibited by the secondary amine functionalized PEGMA-DED amounts
326 to $3.1 \pm 0.2 \cdot 10^{-4} \text{ s}^{-1}$, while that by the PEGMA-EDA amounts to $6.3 \pm 0.4 \cdot 10^{-4} \text{ s}^{-1}$. This

327 observation indicates that, in contrast to when an organic solvent such as hexane is used [4, 7],
328 primary amine sites are more active with water as solvent than the secondary amine sites [11].
329 This has been reported previously by Kandel et al. [11] and is attributed to the presence of water
330 shifting the equilibrium away from the inhibiting imine on primary amines while also promoting
331 the formation of inhibiting iminium ions on secondary amines. While comparison with literature
332 reported turnover frequencies should be performed carefully, due to different reaction conditions,
333 the obtained TOF for the PEGMA-EDA catalyst is 4 times higher than the state-of-the-art
334 primary amine functionalized mesoporous silica catalyst that was evaluated in water [12], and is
335 comparable to the TOF of this primary amine functionalized silica catalyst evaluated in hexane
336 [4]. This difference in activity for both catalysts using water is most likely related to a difference
337 in adsorption behavior in the catalyst pores resulting in a different local polarity environment
338 [12, 41].

339 **Table 2:** Turnover frequency for the PEGMA catalysts in the Parr[®] batch reactor for the aldol reaction of
340 acetone with 4-nitrobenzaldehyde. (T = 55 °C, m_{acetone} = 45 g, m_{4NB} = 0.45 g, m_{water} = 55 g, 0.06 mmol
341 amine sites)

Catalyst	TOF (s ⁻¹)
PEGMA-EDA	6.3 ± 0.4 10 ⁻⁴
PEGMA-DED	3.1 ± 0.2 10 ⁻⁴
PEGMA-MA	0.0

342

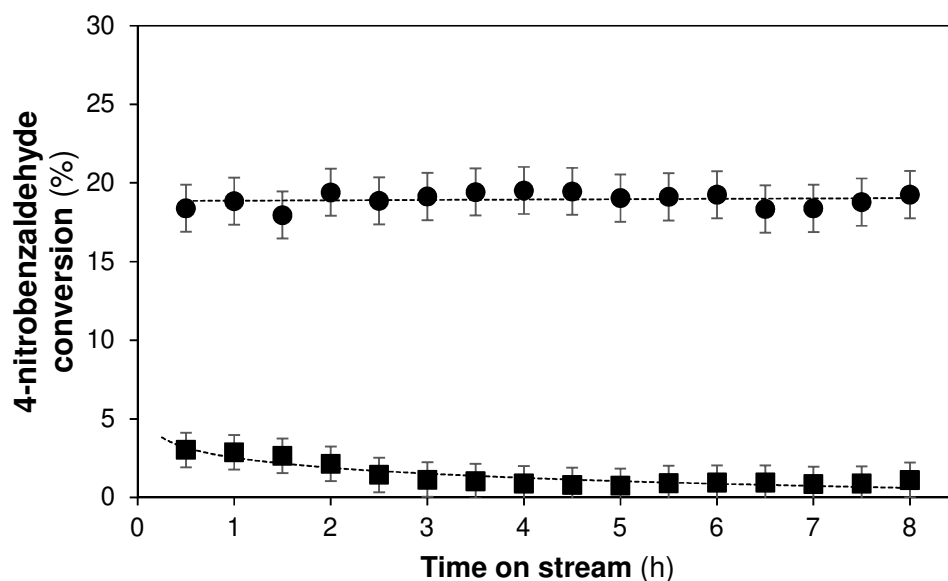
343

344 4.3 Comparison of PEGMA-EDA stability to the state-of-the-art aminated silica

345

346 Reusability of the PEGMA catalysts was not evaluated in the Parr[®] batch reactor because the
347 small resin beads were difficult to completely recover after a first run. To avoid errors while
348 filtering and recycling a catalyst in consecutive batch tests, the stability of the PEGMA-EDA

349 catalyst has been evaluated in a packed-bed plug-flow reactor [28] and is compared at the same
350 reaction conditions, to the stability of the current state-of-the-art primary amine functionalized
351 mesoporous silica catalyst. The catalytic activity, expressed as 4-nitrobenzaldehyde conversion,
352 versus time on stream is displayed in Figure 7 for both catalysts.



353
354 **Figure 7:** Conversion as a function of time on stream for the PEGMA-EDA catalyst (●) and the Silica-
355 APS catalyst (■) in the aldol reaction of acetone with 4-nitrobenzaldehyde. (T = 55 °C, P = 180 kPa, site
356 time = 544 mol_{site}.s.mol⁻¹, 0.45 wt% 4-nitrobenzaldehyde, 44.6 wt% acetone, 54.5 wt% water, 0.25 wt%
357 IS.) Line is a guide for the eye.

358
359 The PEGMA-EDA catalyst exhibited a constant conversion as a function of time on stream for at
360 least 8 hours. On the other hand, at these reaction conditions, the state-of-the-art primary amine
361 functionalized mesoporous silica exhibited an initial activity that is almost 4 times lower than
362 that of the PEGMA-EDA catalyst, as could be expected from the TOF results in the batch
363 reactor. Additionally, it can be observed the amine functionalized mesoporous silica loses most
364 of its activity in the first 3 hours on stream, which is likely caused by leaching of the active sites

365 [14, 16]. This is attributed to the large amounts of water present in the reactor. Clearly, these
366 reaction conditions are far from optimal for the activity and stability of the Silica-APS catalysts
367 in the aldol reaction. However, water was previously found to be required for these catalysts to
368 prevent site-blocking species being formed on the amine sites [16]. Yet, deactivation by
369 hydrolysis and subsequent leaching of active sites remained an inherent problem with amine
370 functionalized mesoporous silica catalysts. This was shown in our previous experimental work,
371 where a lower water contents in an organic solvent such as DMSO [16] also resulted in
372 deactivation with time on stream, albeit to a lesser extent, *i.e.*, losing about a third of its activity
373 in the first 10 hours on-stream. On the contrary, in this work the PEGMA-EDA catalyst appears
374 to exhibit a much better resistance against deactivation during the aldol reaction even when
375 exposed to high water concentrations. This clearly demonstrates the potential of amine
376 functionalized resin catalysts. Moreover, in contrast to the more widely used polystyrene resin
377 catalysts [29], the catalyst developed in this work sufficiently swells in high-polarity solvents
378 such as water to allow access to the active sites, resulting in a TOF that can rival with the current
379 state-of-the-art materials [4, 12, 31]. Hence, the developed catalyst based on PEGMA resins
380 opens up bright perspectives for future application in reactions using water as solvent.

381 **5 Conclusions**

382 For the first time, a highly active heterogeneous amine catalyst is developed that exhibits a stable
383 activity in the continuous-flow aldol reaction of acetone with 4-nitrobenzaldehyde. The catalyst
384 support material was synthesized via a free radical suspension polymerization of a (poly
385 ethyleneglycol) methacrylate (PEGMA) monomer and poly(ethylene glycol) dimethacrylate
386 (PEGDMA) as cross-linker. Chlorine functionalization of a part of the hydroxyl groups was
387 performed with thionyl chloride. Subsequent amine functionalization was then performed by

388 nucleophilic substitution of different diamines and amines on the partly chlorinated material. The
389 successful chlorination and amine functionalization was confirmed by ^{13}C -NMR and FT-IR
390 measurements, which yielded no indications of undesired side-reactions taking place during the
391 catalyst synthesis. Elemental CHN analysis was performed to quantify the active sites.

392 Functionalization was performed with ethylenediamine (EDA), N,N'-dimethylethylenediamine
393 (DED) and methylamine (MA) respectively resulting in a primary amine catalyst and two
394 secondary amine catalysts. Evaluation of their kinetic performance was done in a batch reactor
395 for the aldol reaction of acetone with 4-nitrobenzaldehyde using 50 vol% water as solvent and 50
396 vol% acetone as excess reagent. The PEGMA-MA catalyst did not exhibit any turnover,
397 indicating that the secondary amine in the backbone of the active site on the PEGMA-EDA
398 catalyst is most likely not contributing to the observed activity. A TOF of $6.3 \pm 0.4 \cdot 10^{-4} \text{ s}^{-1}$ was
399 reported for the PEGMA-EDA catalyst, which is in the same range as the currently best
400 performing promoted heterogeneous amine catalysts that were evaluated in hexane, and 3.1 ± 0.2
401 10^{-4} s^{-1} for the PEGMA-DED catalyst.

402 The most active PEGMA catalyst, i.e. the PEGMA-EDA catalyst, was also evaluated in a
403 packed-bed continuous-flow reactor under the same reaction conditions as the batch reactor and
404 exhibited a stable conversion with time on stream for at least 8 hours, indicating stable catalyst
405 behavior. This is in stark contrast with the current state-of-the-art primary amine functionalized
406 mesoporous silica catalysts which exhibited a lower activity and deactivated completely after
407 only 3 hours on stream under the same reaction conditions. The developed PEGMA-based
408 catalysts, hence, open up new perspectives for the application in continuous-flow aldol reactions
409 using water as solvent.

410 **6 References**

- 411 [1] G. Kelly, F. King, M. Kett, Waste elimination in condensation reactions of industrial importance,
412 *Green Chemistry*, 4 (2002) 392-399.
- 413 [2] S. Nasir Abbas Bukhari, M. Jasamai, I. Jantan, W. Ahmad, Review of methods and various catalysts
414 used for chalcone synthesis, *Mini-Reviews in Organic Chemistry*, 10 (2013) 73-83.
- 415 [3] C. Barrett, J. Chheda, G. Huber, J. Dumesic, Single-reactor process for sequential aldol-condensation
416 and hydrogenation of biomass-derived compounds in water, *Applied Catalysis B: Environmental*, 66
417 (2006) 111-118.
- 418 [4] J. Lauwaert, E. De Canck, D. Esquivel, P. Van Der Voort, J.W. Thybaut, G.B. Marin, Effects of amine
419 structure and base strength on acid–base cooperative aldol condensation, *Catalysis Today*, 246 (2015) 35-
420 45.
- 421 [5] N.A. Brunelli, C.W. Jones, Tuning acid–base cooperativity to create next generation silica-supported
422 organocatalysts, *Journal of Catalysis*, 308 (2013) 60-72.
- 423 [6] Y. Kubota, K. Goto, S. Miyata, Y. Goto, Y. Fukushima, Y. Sugi, Enhanced Effect of Mesoporous
424 Silica on Base-Catalyzed Aldol Reaction, *Chemistry Letters*, 32 (2003) 234-235.
- 425 [7] K. Kandel, S.M. Althaus, C. Peeraphatdit, T. Kobayashi, B.G. Trewyn, M. Pruski, I.I. Slowing,
426 Substrate inhibition in the heterogeneous catalyzed aldol condensation: A mechanistic study of supported
427 organocatalysts, *Journal of Catalysis*, 291 (2012) 63-68.
- 428 [8] R.K. Zeidan, S.J. Hwang, M.E. Davis, Multifunctional Heterogeneous Catalysts: SBA-15-Containing
429 Primary Amines and Sulfonic Acids, *Angewandte Chemie International Edition*, 45 (2006) 6332-6335.
- 430 [9] J. Lauwaert, E.G. Moschetta, P. Van Der Voort, J.W. Thybaut, C.W. Jones, G.B. Marin, Spatial
431 arrangement and acid strength effects on acid–base cooperatively catalyzed aldol condensation on
432 aminosilica materials, *Journal of Catalysis*, 325 (2015) 19-25.
- 433 [10] A. De Vylder, J. Lauwaert, M.K. Sabbe, M.-F. Reyniers, J. De Clercq, P. Van Der Voort, J.W.
434 Thybaut, Rational design of nucleophilic amine sites via computational probing of steric and electronic
435 effects, *Catalysis Today*, 334 (2019) 96-103.
- 436 [11] K. Kandel, S.M. Althaus, C. Peeraphatdit, T. Kobayashi, B.G. Trewyn, M. Pruski, I.I. Slowing,
437 Solvent-Induced Reversal of Activities between Two Closely Related Heterogeneous Catalysts in the
438 Aldol Reaction, *ACS Catalysis*, 3 (2013) 265-271.
- 439 [12] D. Singappuli-Arachchige, T. Kobayashi, Z. Wang, S.J. Burkhaw, E.A. Smith, M. Pruski, I.I.
440 Slowing, Interfacial Control of Catalytic Activity in the Aldol Condensation: Combining the Effects of
441 Hydrophobic Environments and Water, *ACS Catalysis*, (2019).
- 442 [13] M.-O. Simon, C.-J. Li, Green chemistry oriented organic synthesis in water, *Chemical Society*
443 *Reviews*, 41 (2012) 1415-1427.
- 444 [14] M. Etienne, A. Walcarius, Analytical investigation of the chemical reactivity and stability of
445 aminopropyl-grafted silica in aqueous medium, *Talanta*, 59 (2003) 1173-1188.

- 446 [15] E. Asenath Smith, W. Chen, How to prevent the loss of surface functionality derived from
447 aminosilanes, *Langmuir*, 24 (2008) 12405-12409.
- 448 [16] A. De Vylder, J. Lauwaert, D. Esquivel, D. Poelman, J. De Clercq, P. Van Der Voort, J.W. Thybaut,
449 The role of water in the reusability of aminated silica catalysts for aldol reactions, *Journal of Catalysis*,
450 361 (2018) 51-61.
- 451 [17] F. Giacalone, M. Gruttadauria, A.M. Marculescu, R. Noto, Polystyrene-supported proline and
452 prolinamide. Versatile heterogeneous organocatalysts both for asymmetric aldol reaction in water and α -
453 selenenylation of aldehydes, *Tetrahedron letters*, 48 (2007) 255-259.
- 454 [18] D. Font, C. Jimeno, M.A. Pericas, Polystyrene-supported hydroxyproline: An insoluble, recyclable
455 organocatalyst for the asymmetric aldol reaction in water, *Organic letters*, 8 (2006) 4653-4655.
- 456 [19] M. Gruttadauria, F. Giacalone, A. Mossuto Marculescu, P. Lo Meo, S. Riela, R. Noto,
457 Hydrophobically Directed Aldol Reactions: Polystyrene-Supported L-Proline as a Recyclable Catalyst for
458 Direct Asymmetric Aldol Reactions in the Presence of Water, *European Journal of Organic Chemistry*,
459 2007 (2007) 4688-4698.
- 460 [20] M. Gruttadauria, A.M.P. Salvo, F. Giacalone, P. Agrigento, R. Noto, Enhanced activity and
461 stereoselectivity of polystyrene-supported proline-based organic catalysts for direct asymmetric aldol
462 reaction in water, *European Journal of Organic Chemistry*, 2009 (2009) 5437-5444.
- 463 [21] K. Akagawa, S. Sakamoto, K. Kudo, Direct asymmetric aldol reaction in aqueous media using
464 polymer-supported peptide, *Tetrahedron letters*, 46 (2005) 8185-8187.
- 465 [22] P. Llanes, S. Sayalero, C. Rodríguez-Escrich, M.A. Pericàs, Asymmetric cross-and self-aldol
466 reactions of aldehydes in water with a polystyrene-supported triazolylproline organocatalyst, *Green*
467 *Chemistry*, 18 (2016) 3507-3512.
- 468 [23] G. Guo, Y. Wu, X. Zhao, J. Wang, L. Zhang, Y. Cui, Polymerization of L-proline functionalized
469 styrene and its catalytic performance as a supported organocatalyst for direct enantioselective aldol
470 reaction, *Tetrahedron: Asymmetry*, 27 (2016) 740-746.
- 471 [24] A. del Prado, M. Pintado-Sierra, M. Juan-y-Seva, R. Navarro, H. Reinecke, J. Rodríguez-Hernández,
472 C. Elvira, A. Fernández-Mayoralas, A. Gallardo, Aqueous micro and nanoreactors based on alternating
473 copolymers of phenylmaleimide and vinylpyrrolidone bearing pendant l-proline stabilized with PEG
474 grafted chains, *Journal of Polymer Science Part A: Polymer Chemistry*, 55 (2017) 1228-1236.
- 475 [25] N. Mase, Y. Nakai, N. Ohara, H. Yoda, K. Takabe, F. Tanaka, C.F. Barbas, Organocatalytic direct
476 asymmetric aldol reactions in water, *Journal of the American Chemical Society*, 128 (2006) 734-735.
- 477 [26] S.L. Scott, *A Matter of Life (time) and Death*, in, ACS Publications, 2018.
- 478 [27] C.W. Jones, On the stability and recyclability of supported metal–ligand complex catalysts: myths,
479 misconceptions and critical research needs, *Topics in Catalysis*, 53 (2010) 942-952.
- 480 [28] A. De Vylder, J. Lauwaert, S. Van Auwenis, J. De Clercq, J.W. Thybaut, Catalyst Stability
481 Assessment in a Lab-Scale Liquid Solid (LS)² Plug-Flow Reactor, *Catalysts*, (2019).

- 482 [29] C.B. Hoyt, L.C. Lee, A.E. Cohen, M. Weck, C.W. Jones, Bifunctional Polymer Architectures for
483 Cooperative Catalysis: Tunable Acid–Base Polymers for Aldol Condensation, *ChemCatChem*, 9 (2017)
484 137-143.
- 485 [30] N.C. Ellebracht, C.W. Jones, Amine functionalization of cellulose nanocrystals for acid–base
486 organocatalysis: surface chemistry, cross-linking, and solvent effects, *Cellulose*, 25 (2018) 6495-6512.
- 487 [31] N.C. Ellebracht, C.W. Jones, Optimized Cellulose Nanocrystal Organocatalysts Outperform Silica-
488 Supported Analogues: Cooperativity, Selectivity, and Bifunctionality in Acid–Base Aldol Condensation
489 Reactions, *ACS Catalysis*, 9 (2019) 3266-3277.
- 490 [32] A. De Vylder, J. Lauwaert, J. De Clercq, P. Van Der Voort, C.V. Stevens, J.W. Thybaut, Kinetic
491 evaluation of chitosan-derived catalysts for the aldol reaction in water, *Reaction Chemistry &*
492 *Engineering*, (2019).
- 493 [33] E. Van de Steene, J. De Clercq, J.W. Thybaut, Ion-exchange resin catalyzed transesterification of
494 ethyl acetate with methanol: Gel versus macroporous resins, *Chemical Engineering Journal*, 242 (2014)
495 170-179.
- 496 [34] J.M. Harris, Introduction to biotechnical and biomedical applications of poly (ethylene glycol), in:
497 *Poly (ethylene glycol) Chemistry*, Springer, 1992, pp. 1-14.
- 498 [35] W. Rapp, PEG grafted polystyrene tentacle polymers: Physicochemical properties and application in
499 chemical synthesis, VCH: Weinheim, 1996.
- 500 [36] J.M. Harris, Laboratory synthesis of polyethylene glycol derivatives, *Journal of Macromolecular*
501 *Science-Reviews in Macromolecular Chemistry and Physics*, 25 (1985) 325-373.
- 502 [37] A. Tuncel, Suspension polymerization of poly (ethylene glycol) methacrylate: a route for swellable
503 spherical gel beads with controlled hydrophilicity and functionality, *Colloid and Polymer Science*, 278
504 (2000) 1126-1138.
- 505 [38] N.A. Brunelli, K. Venkatasubbaiah, C.W. Jones, Cooperative catalysis with acid–base bifunctional
506 mesoporous silica: impact of grafting and co-condensation synthesis methods on material structure and
507 catalytic properties, *Chemistry of Materials*, 24 (2012) 2433-2442.
- 508 [39] P. Van Der Voort, E. Vansant, Silylation of the silica surface a review, *Journal of liquid*
509 *chromatography & related technologies*, 19 (1996) 2723-2752.
- 510 [40] B. List, R.A. Lerner, C.F. Barbas, Proline-catalyzed direct asymmetric aldol reactions, *Journal of the*
511 *American Chemical Society*, 122 (2000) 2395-2396.
- 512 [41] D. Singappuli-Arachchige, J.S. Manzano, L.M. Sherman, I.I. Slowing, Polarity Control at Interfaces:
513 Quantifying Pseudo-solvent Effects in Nano-confined Systems, *ChemPhysChem*, 17 (2016) 2982-2986.

514

515 ASSOCIATED CONTENT

516 **Supporting Information**

517 The following files are available free of charge.

- 518 • Supporting Information containing additional characterization of the catalysts (PDF)

519 AUTHOR INFORMATION

520 **Corresponding Author**

521 *Joris W. Thybaut (Joris.Thybaut@UGent.be)

522 **Author Contributions**

523 The manuscript was written through contributions of all authors. All authors have given approval
524 to the final version of the manuscript.

525 ACKNOWLEDGMENT

526 The authors acknowledge financial support from the Research Foundation - Flanders (FWO)
527 through Grant Number V401719N and the European Research Council under the European
528 Union's Seventh Framework Programme (FP7/2007-2013) / ERC grant agreement n°615456.
529 J.L. is a postdoctoral fellow of the Research Foundation - Flanders (12Z2218N). C.W.J.
530 acknowledges support from the United States Department of Energy, Basic Energy Sciences
531 through Catalysis Science contract DE-FG02-03ER15459.

Graphical Abstract

